Direct numerical simulation of flexible molecules and data-driven molecular conformation

Amine Ammar [a,*], Francisco Chinesta [b]

[a] LAMPA @ Arts et Métiers ParisTech, 2, boulevard du Ronceray, BP 93525, 49035 Angers cedex 01, France

[b] ESI Group Chair @ PIMM, Arts et Métiers Institute of Technology, CNRS, CNAM, HESAM University, 151 boulevard de l'Hôpital, 75013 Paris, France

A B S T R A C T

The present work aims at performing a molecular dynamics modeling of suspensions composed of flexible linear molecules. Molecules are represented by a series of connected beads, whose dynamics is governed by three potentials: the extension potential affecting the elongation of segments connecting consecutive beads, the one governing the molecule bending and finally the Lennard-Jones describing the interaction of non-consecutive beads. A population of non-interacting molecules is simulated in elongation and shear flows for different flow and molecule parameters. The flow-induced conformation is analyzed in the different considered situations. Finally a model for predicting the evolution of the population conformation will be obtained by using deep-learning.

Keywords:
Flexible molecules
Direct numerical simulation
Molecular dynamics
Suspension
Deep-learning

1. Introduction

Polymers and viscoelastic fluids can be described at different scales, deeply discussed in many books, among them [1] [2]. The molecular scale (see [3] [4] and the references therein) precedes the one of kinetic theory where the molecules individuality is replaced by a scalar distribution function – DF – involving a series of conformational coordinates [2]. Most of kinetic theory models represent molecules as multi-bead-rod or multi-bead-springs idealizations, usually coarsened by using the end-to-end vector to reduce the dimensionality of the conformational space [5]. The resulting models were in general solved numerically by using Brownian and stochastic numerical techniques for circumventing the so-called curse of dimensionality that the high-dimensionality of the conformation space entails [6] [7].

In [8] and [9] authors consider Gaussian chains combined with the Langevin equation for better account for the molecular conformation. Works attaining the atomic scale are quite scare, being the resulting models difficult to extend to larger scales [10–14].

The present work aims at performing a molecular dynamics modeling of suspensions composed of flexible molecules. Such a description scale has as main advantage the fine representation of the molecular configurations, finer than the ones attainable when using coarser descriptions (e.g. kinetic theory descriptions). The main drawback when using these extremely fine descriptions concerns the computational cost. However, to have access to the real behavior and evaluate the validity of coarser descriptions, high fidelity simulations at the finest scale seems compulsory. Moreover, as soon as an accurate approximation of the microscopic physics is attained and available, it could be then introduced into coarser descriptions.

* Corresponding author.
E-mail addresses: Amine.AMMAR@ensam.eu (A. Ammar), Francisco.CHINESTA@ensam.eu (F. Chinesta).

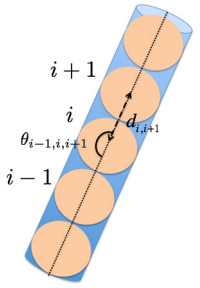

Fig. 1. Molecule schema.

When describing finely molecules as a series of connected beads, the whole molecular conformation strongly depends on the choice of the potentials used for deriving the forces to be introduced into the motion equation at the beads level. Different potentials are in general considered: (i) the one describing the extension of the inter-beads segment; (ii) the one describing the molecule bending mechanism, that is expressed at each bead from its two neighbors; and finally (iii) the weak interaction (Lennard-Jones) between non-neighbor beads. The evaluation of the population conformation with respect to the different available choice of potentials and in particular their intensity is of major interest to better describe rheological features. In the present work and without loss of generality of the proposed methodology we consider dilute suspensions, that allows neglecting the interaction of beads belonging to different molecules.

Our model assumes linear molecules composed of beads at which, other than the potentials just discussed, also acts Brownian events representing the action of the molecules of solvent in which the molecule is assumed be immersed. A population of non-interacting molecules is simulated in elongation and shear flows for different flow and molecule parameters. The flow-induced conformation is analyzed in the different considered situations and some statistical outputs extracted.

Finally a model for predicting the evolution of the population conformation will be obtained by using deep-learning, deeply used in a variety of applications, as system control [15,16] and dynamical systems [17] for citing few.

2. Fine-scale discrete simulation

The fine scale simulation is performed by representing the molecule as a series of connected beads where forces apply, the last derived from different potentials as well as the bombardment of solvent molecules.

As previously discussed we are considering three different potentials responsible of three different deformation mechanisms: the Lennard-Jones potential V^{LJ} is used to describe the inter-beads interactions (of non-neighbor beads), and other two potentials, V^{E} and V^{B}, are used to describe the molecule segments elongations and chain bending respectively, see Fig. 1.

Thus, the total potential reads

$$V = \sum_{j=1}^{\mathtt{M}} \sum_{i=1}^{\mathtt{N}-1} V^{\mathrm{E}}_{i,i+1;\,j} + \sum_{j=1}^{\mathtt{M}} \sum_{i=2}^{\mathtt{N}-1} V^{\mathrm{B}}_{i-1,i,i+1;\,j} + \sum_{j=1}^{\mathtt{M}} \sum_{i=1}^{\mathtt{N}} \sum_{k=1}^{\mathtt{N}} V^{\mathrm{LJ}}_{i,k;\,j}\chi_{ik;\,j} \tag{1}$$

where $\mathtt{M}$ is the number of molecules in the population, j refers to the molecule chain in that population, and i refers to the considered bead composing it, $i = 1, \ldots, \mathtt{N}$ (with $\mathtt{N}$ the number of beads composing the molecular chain). Finally we define a characteristic function for describing the bead direct neighborhood: $\chi_{ik} = 1$ if $|i-k| > 1$ and $\chi_{ik} = 0$ if $|i-k| \leq 1$

The Lennard-Jones potential reads

$$V^{\mathrm{LJ}}_{i,k} = 4\varepsilon \left(\left(\frac{\sigma}{d_{ik}} \right)^{12} - \left(\frac{\sigma}{d_{ik}} \right)^{6} \right) \tag{2}$$

with $d_{ik} = ||\mathbf{x}_k - \mathbf{x}_i||$ the distance between beads $\mathcal{B}_i$ and $\mathcal{B}_k$, located at positions $\mathbf{x}_i$ and $\mathbf{x}_k$ respectively, and ϵ and σ the two usual parameters involved in the Lennard-Jones potential.

The elongation potential is given by

$$V^{\mathrm{E}}_{i,i+1} = \frac{K_{\mathrm{E}}}{2} \left(1 - \frac{d_{ij}}{d_{\mathrm{eq}}} \right)^2 \tag{3}$$

where d_{eq} is the equilibrium distance between two successive beads, distance at which the potential reaches its minimum (and consequently the associated force vanishes). In the previous expression K_{E} reflects the potential intensity.

The bending potential between three successive beads

$$V^{\mathrm{B}}_{i-1,i,i+1} = \frac{K_{\mathrm{B}}}{2} \left(\theta_{i-1,i,i+1} - \theta_{\mathrm{eq}} \right)^2 \tag{4}$$

where $\theta_{i-1,i,i+1}$ is the angle defined by vectors joining beads $i-1, i$ and $i, i+1$ with θ_{eq} the angle at equilibrium. In our study we consider $\theta_{\text{eq}} = 70.5°$ (that corresponds to the angle between two consecutive carbone-carbone bonds). Again, the potential intensity is described from K_{B}.

The force applying at each bead related to these three molecule deformation mechanisms results from the potential derivative according to

$$\mathbf{F}_i^{\text{I}} = -\frac{\partial V}{\partial \mathbf{x}_i} \tag{5}$$

There are two other forces acting on the bead. First, the one related to the fluid drag $\mathbf{F}_i^{\text{D}}$. Let $\mathbf{v}(\mathbf{x})$ be the fluid velocity at position $\mathbf{x}$, assumed unperturbed by the rods presence, the drag force reads

$$\mathbf{F}_i^{D} = \xi(\mathbf{v}(\mathbf{x}_i) - \dot{\mathbf{x}}_i) \tag{6}$$

where $\dot{\mathbf{x}}_i$ denotes the velocity of bead $\mathcal{B}_i$.

Finally a Brownian force is also considered emulating the solvent bombardment, and is expressed from

$$\mathbf{F}_i^{\text{Brow}} = \sqrt{2D\,\text{d}t}\,W_i \tag{7}$$

where D denotes the diffusion coefficient, dt the calculation time step and W_i a random variable with zero mean and unit standard deviation.

The linear momentum balance involving bead $\mathcal{B}_i$ reads

$$\mathbf{F}_i = \mathbf{F}_i^{D} + \mathbf{F}_i^{I} + \mathbf{F}_i^{\text{Brow}} = m\,\mathbf{a}_i \tag{8}$$

with the particle acceleration $\mathbf{a}_i = \frac{\text{d}\dot{\mathbf{x}}_i}{\text{d}t} = \frac{\text{d}^2\mathbf{x}_i}{\text{d}t^2}$.

A second-order time integration scheme is considered, consisting of

$$\begin{cases} \mathbf{a}_i^{n+1} = \frac{\mathbf{F}_i^n}{m} \\ \mathbf{x}_i^{n+1} = \mathbf{x}_i^n + \dot{\mathbf{x}}_i^n \Delta t + \frac{1}{2}\mathbf{a}_i(t)(\Delta t)^2 \\ \dot{\mathbf{x}}_i^{n+1} = \dot{\mathbf{x}}_i^n + \frac{1}{2}\left(\mathbf{a}_i^n + \mathbf{a}_i^{n+1}\right)\Delta t \end{cases} \tag{9}$$

where the superscript n refers to the time step, $t_n = n\Delta t$.

Prior to proceed with the time integration, equations are rewritten in dimensionless form, by considering as characteristic variables

- length: σ
- energy: ε
- mass: m
- velocity: $\sqrt{\varepsilon/m}$
- acceleration: $\varepsilon/(m\sigma)$
- time: $\sigma\sqrt{m/\varepsilon}$
- diffusion: $\sigma^{-3}\sqrt{\frac{\epsilon^5}{m}}$

which allows writing the dimensionless model in which, for the sake of clarity, we do not change the notation for designating the dimensionless variables.

Thus, we obtain

$$\begin{cases} V_{i,j}^{\text{LJ}} = 4\left(\left(\frac{1}{d_{ij}}\right)^{12} - \left(\frac{1}{d_{ij}}\right)^{6}\right) \\ V_{i,i+1}^{\text{E}} = \frac{\hat{K}_{\text{E}}}{2}\left(1 - \frac{d_{ij}}{d_{\text{eq}}}\right)^2 \\ V_{i-1,i,i+1}^{\text{B}} = \frac{\hat{K}_{\text{B}}}{2}(\theta_{i-1,i,i+1} - \theta_{\text{eq}})^2 \\ \mathbf{F}_i^{I} = -\frac{\partial V}{\partial \mathbf{x}_i} \\ \mathbf{F}_i^{D} = \hat{\xi}(\mathbf{v}(\mathbf{x}_i) - \dot{\mathbf{x}}_i) \\ \mathbf{F}_i^{\text{Brow}} = \sqrt{2\hat{D}\widehat{\text{d}t}}W_i \\ \mathbf{F}_i = \mathbf{a}_i \end{cases} \tag{10}$$

where $\hat{K}_{\text{E}} = \frac{K_{\text{E}}}{\varepsilon}$, $\hat{K}_{\text{B}} = \frac{K_{\text{B}}}{\varepsilon}$, $\hat{\xi} = \xi\sqrt{\varepsilon m}/\sigma$, $\hat{D} = D\sigma^3\sqrt{\frac{m}{\epsilon^5}}$ and $\widehat{\text{d}t} = \frac{\text{d}t}{\sigma}\sqrt{\frac{\epsilon}{m}}$.

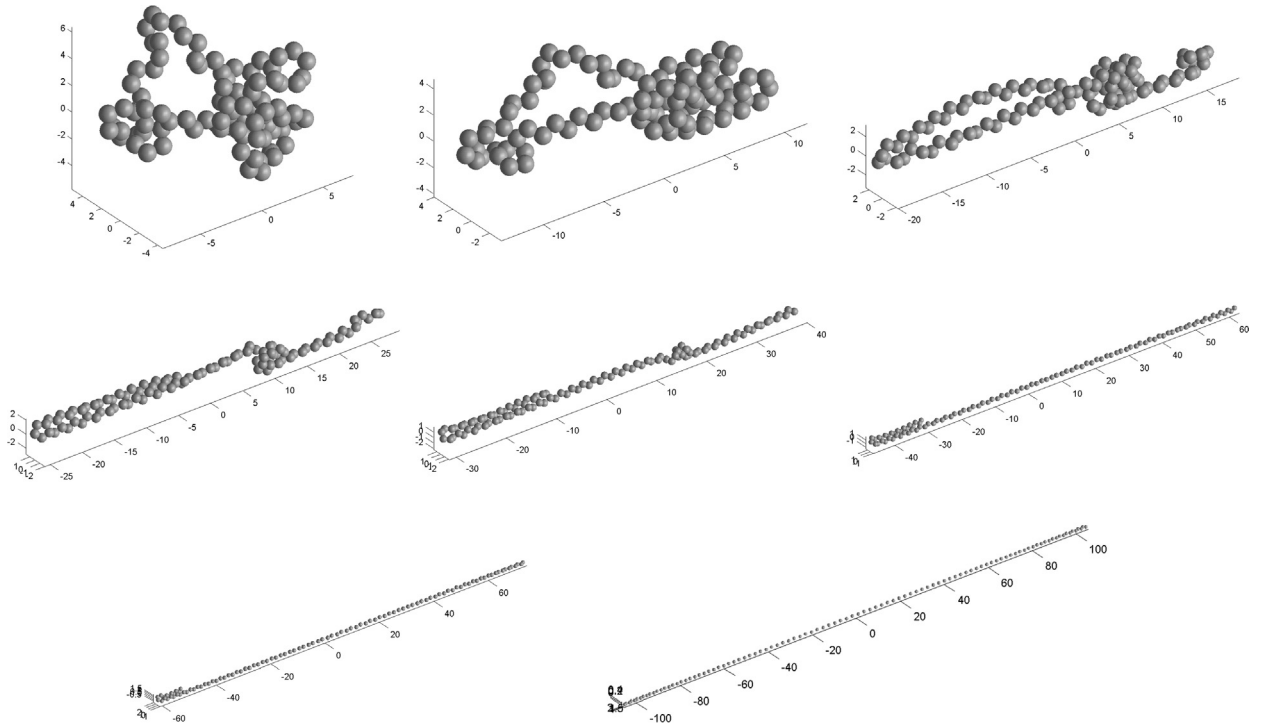

Fig. 2. Initial conformation and its evolution when subjected to elongation.

3. Results

In the numerical results reported in the present section we assumed as equilibrium distance between two consecutive beads the one associated with the Lennard-Jones (dimensionless) potential, i.e. $d_{\text{eq}} = 2^{1/6}$. In order to avoid large fluctuations of the molecule length we assume a quite large elongation stiffness $\hat{K}_{\text{E}} = 10000$ and a bending potential $\hat{K}_{\text{B}} = 1000$.

In order to derive rheological properties (based on the molecular conformation), a large enough population of molecules must be considered, allowing one to compute accurate statistics. In the cases reported in the present paper $\mathtt{M} = 1000$ chains involving $\mathtt{N}$ beads, $\mathtt{N} = 100$, and consequently 99 inter-bead segments are considered. In all cases the dimensionless diffusion and drag coefficients were assumed taking unit values.

Two simple rheological flows were addressed, elongational and simple shear flows, both expressed from the dimensionless effective strain rate $\dot{\epsilon}$, leading to the following dimensionless velocity fields:

– elongational flow,

$$\mathbf{v} = \begin{pmatrix} v_x \\ v_y \\ v_z \end{pmatrix} = \begin{pmatrix} \dot{\epsilon} x \\ -\frac{1}{2}\dot{\epsilon} y \\ -\frac{1}{2}\dot{\epsilon} z \end{pmatrix} \tag{11}$$

– simple shear flow,

$$\mathbf{v} = \begin{pmatrix} v_x \\ v_y \\ v_z \end{pmatrix} = \begin{pmatrix} \dot{\epsilon} z \\ 0 \\ 0 \end{pmatrix} \tag{12}$$

where three values of $\dot{\epsilon}$ will be evaluated: (i) $\dot{\epsilon} = 5$; (ii) $\dot{\epsilon} = 1$, and (iii) $\dot{\epsilon} = 0.2$.

The initial state consists of the $\mathtt{M}$=1000 molecules generated randomly. For that purpose the first bead of each chain is place at point $\mathbf{x}_1$. Then the second bead is randomly placed at point $\mathbf{x}_2$ by ensuring $\|\mathbf{x}_2 - \mathbf{x}_1\| = d_{\text{eq}}$. The third bead is place at point $\mathbf{x}_3$ ensuring now the two conditions: (i) $\|\mathbf{x}_3 - \mathbf{x}_2\| = d_{\text{eq}}$ and (ii) $\widehat{\mathbf{L}_{12}\mathbf{L}_{23}} = \theta_{\text{eq}}$, with $\mathbf{L}_{i,i+1} = \mathbf{x}_{i+1} - \mathbf{x}_i$. The procedure continues until placing the final bead.

By proceeding like this, there is the risk that beads in the same molecule approach too much. Thus, before applying the flow, the molecules population is subjected to the Lennard-Jones potential to ensure the fulfillment of the excluded volume. Fig. 2 depicts the initial molecule conformation and then, the one that results from its elongation.

3.1. Case studies

In what follows different analyses are performed by varying the flow and its intensity (elongation and simple shear, with $\dot{\epsilon} = 5$ and $\dot{\epsilon} = 0.2$). Each simulation leads to a figure composed of 8 subfigures, each one representing (top to bottom, left to right):

- representation of the molecules population where the molecule barycentre is placed at the origin of the coordinate system;
- average of the different molecule segments joining consecutive beads (from 1 to $\mathtt{N}-1$);
- the orientation tensor calculated by defining

$$\mathbf{u}^j_{i,i+1} = \frac{\mathbf{L}^j_{i,i+1}}{\|\mathbf{L}^j_{i,i+1}\|} \tag{13}$$

  where j refers the considered molecule in the population, $j = 1, \ldots, \mathtt{M}$, and i the considered bead, $i = 1, \ldots, \mathtt{N}-1$, from which the orientation tensor writes

$$\mathbf{S} = \frac{1}{\mathtt{M}} \sum_{j=1}^{\mathtt{M}} \sum_{i=1}^{\mathtt{N}-1} \mathbf{u}^j_{i,i+1} \otimes \mathbf{u}^j_{i,i+1} \tag{14}$$

- the conformation tensor $\mathbf{C}$ computed from the end-to-end vector $\mathbf{L}^j_{1,\mathtt{N}}$ according to

$$\mathbf{C} = \frac{1}{\mathtt{M}} \sum_{j=1}^{\mathtt{M}} \mathbf{L}^j_{1,\mathtt{N}} \otimes \mathbf{L}^j_{1,\mathtt{N}} \tag{15}$$

- the distribution of $\mathbf{u}^j_{i,i+1}$ on the unit sphere (noted as DF in the figure), each vector being associated with a Gaussian distribution for smoothing the representation;
- a similar representation but now concerning only the end-to-end vectors $\mathbf{u}^j_{1,\mathtt{N}}$;
- average of the segments of all molecules with the associated standard deviation;
- average of segments located at the molecule ends and at the center with their associated standard deviations.

3.2. Discussion

Figs. 3 and 4 concern elongation. It can be noticed that central segments are very elongated, with a final length that at high elongation doubles the one of segments located at the molecules extremities. When decreasing the elongation intensity central segments become less extended, and the end-to-end conformation remains aligned with the elongation, however the segments orientation distribution exhibits a particular annular distribution whose radius depends on the elongation intensity.

Figs. 5 and 6 concern shear flow. Segments have approximately the same length at the almost steady state. An overshoot is noticed at the central segments during the transient regime. At high shear rates the distribution concentrate at two regions (4 by symmetry) that attenuates when decreasing the shear rate.

3.3. Deriving a model of the conformation evolution

As discussed in the introduction section direct numerical simulations are very expensive from the computational point of view, and in that case equations describing the conformation evolution depending on the conformation and the applied flow kinematics seems preferable.

As this kind of model is quite difficult to obtain, here we propose using deep-learning techniques for that purpose. The conformation evolution is assumed evolving according to

$$\frac{\mathrm{d}\mathbf{C}}{\mathrm{d}t} = \mathbf{f}(\mathbf{C}, \nabla\mathbf{v}) \tag{16}$$

with the velocity gradient given by

$$\nabla\mathbf{v} = \begin{pmatrix} \nabla\mathbf{v}_{11} & \nabla\mathbf{v}_{12} & 0 \\ 0 & -\frac{\nabla\mathbf{v}_{11}}{2} & 0 \\ 0 & 0 & -\frac{\nabla\mathbf{v}_{11}}{2} \end{pmatrix} \tag{17}$$

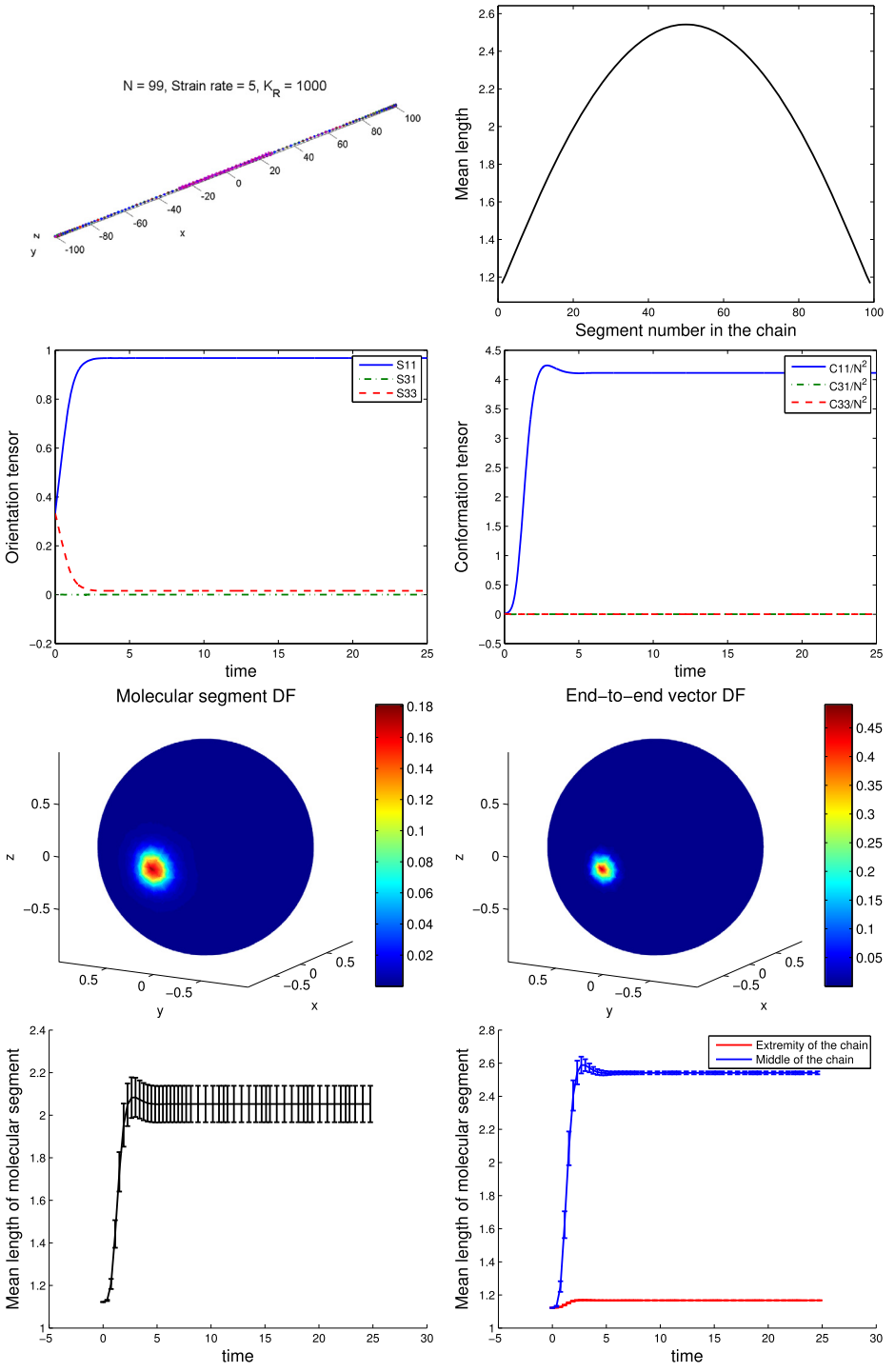

Fig. 3. Elongation at $\dot{\epsilon} = 5$.

We elaborated a neural network – NN – involving two hidden layers of 20 neurons, being the inputs the 6 components of the (symmetric) conformation tensor and the two components of the velocity gradient $\nabla \mathbf{v}_{11}$ and $\nabla \mathbf{v}_{12}$, being the outputs the six components of time derivative of the conformation tensor.

We restrict to molecules composed of 20 beads, i.e. $\mathrm{N} = 20$, with the lower bending stiffness $\hat{K}_{\mathrm{R}} = 100$. 600 flow induced conformations are simulated by choosing randomly both gradient of velocity components, according with the $10^{1.4(\omega - 0.5)}$, where ω is a random variable uniformly distributed in the interval $[0, 1]$. This choice allows ensuring values of the effective strain rate in the interval $(0.2, 5)$, covered almost uniformly in the logarithmic scale.

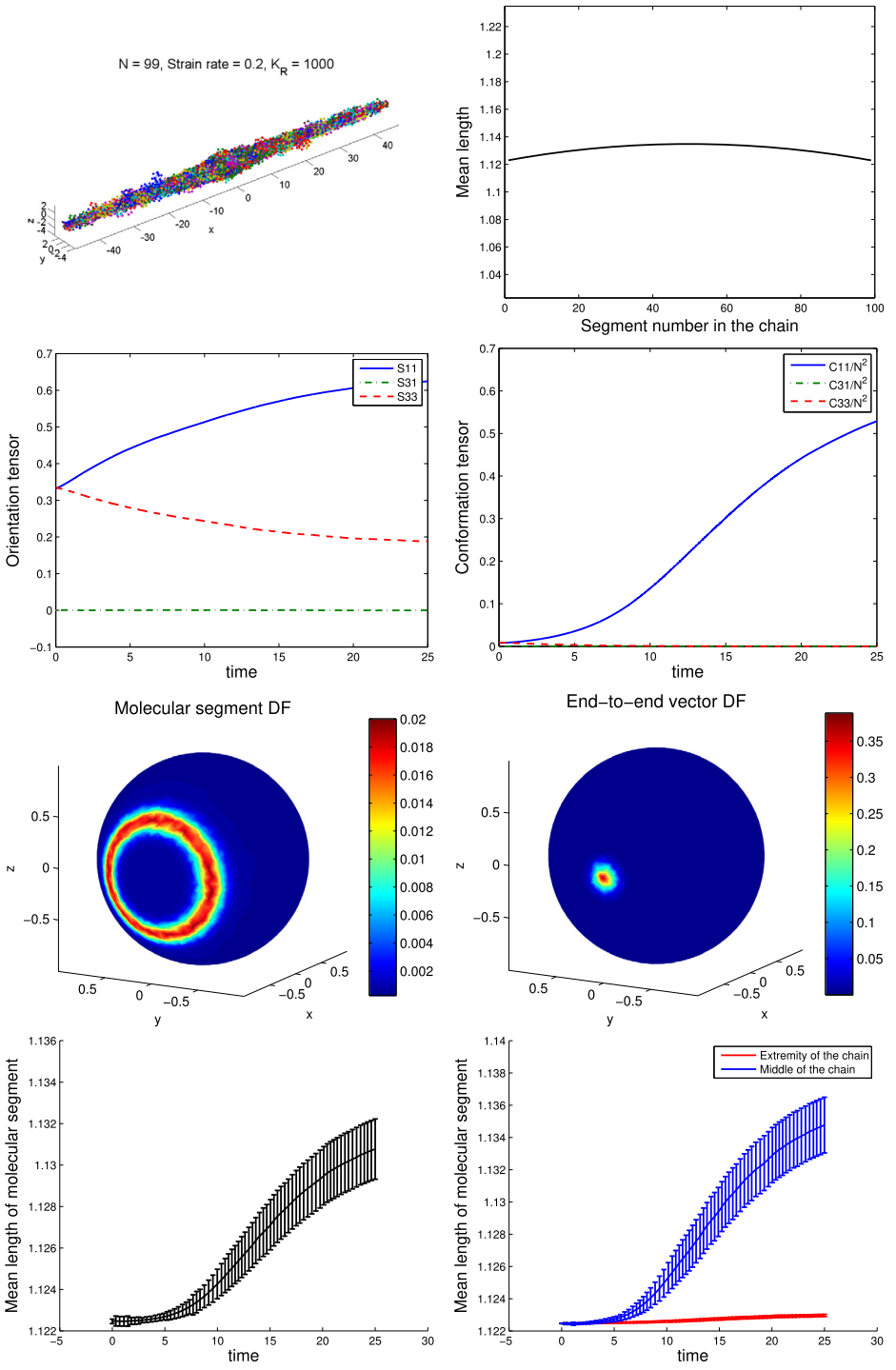

Fig. 4. Elongation at $\dot{\epsilon} = 0.2$.

When the neural network extract the internal weights, the solution is computed again for different values of velocity gradient, randomly chosen, in order to compare the direct numerical solution with the neural-network predictions. Fig. 7 compares both conformation predictions. The conformational predictions are qualitatively in agreement with the ones derived from direct numerical simulations, however quantitatively some gaps are noticed. For reducing them, different routes exist: consider alternative networks, increasing the number of hidden layers or the number of nodes (neurons) in those layers. However, those choices are detrimental with respect to the training efficiency. A deeper comprehension of NN seems necessary for better representing the subjacent physics, to better perform predictions while keeping as reduced as possible

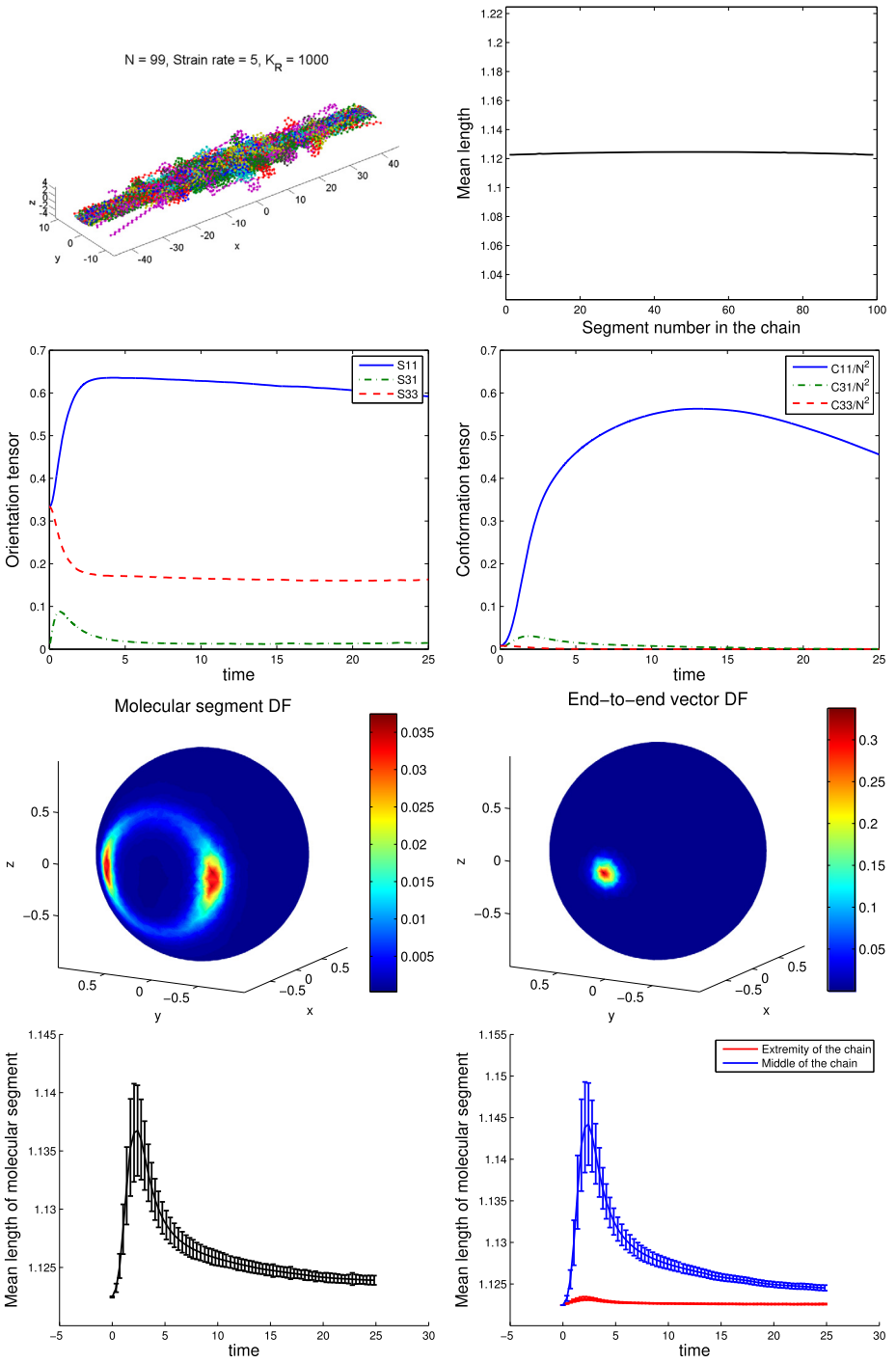

Fig. 5. Shear at $\dot{\epsilon} = 5$.

the training needs (it is important to note that direct numerical simulations that serve for training the NN are extremely expensive from the computational viewpoint).

4. Conclusion

In this paper, we proposed a direct numerical simulation of a suspension of non-interacting flexible molecules, and evaluated the flow induced conformation. Simulations prove that the conformation can exhibit unexpected features, as the annular distribution of the molecular segments orientation.

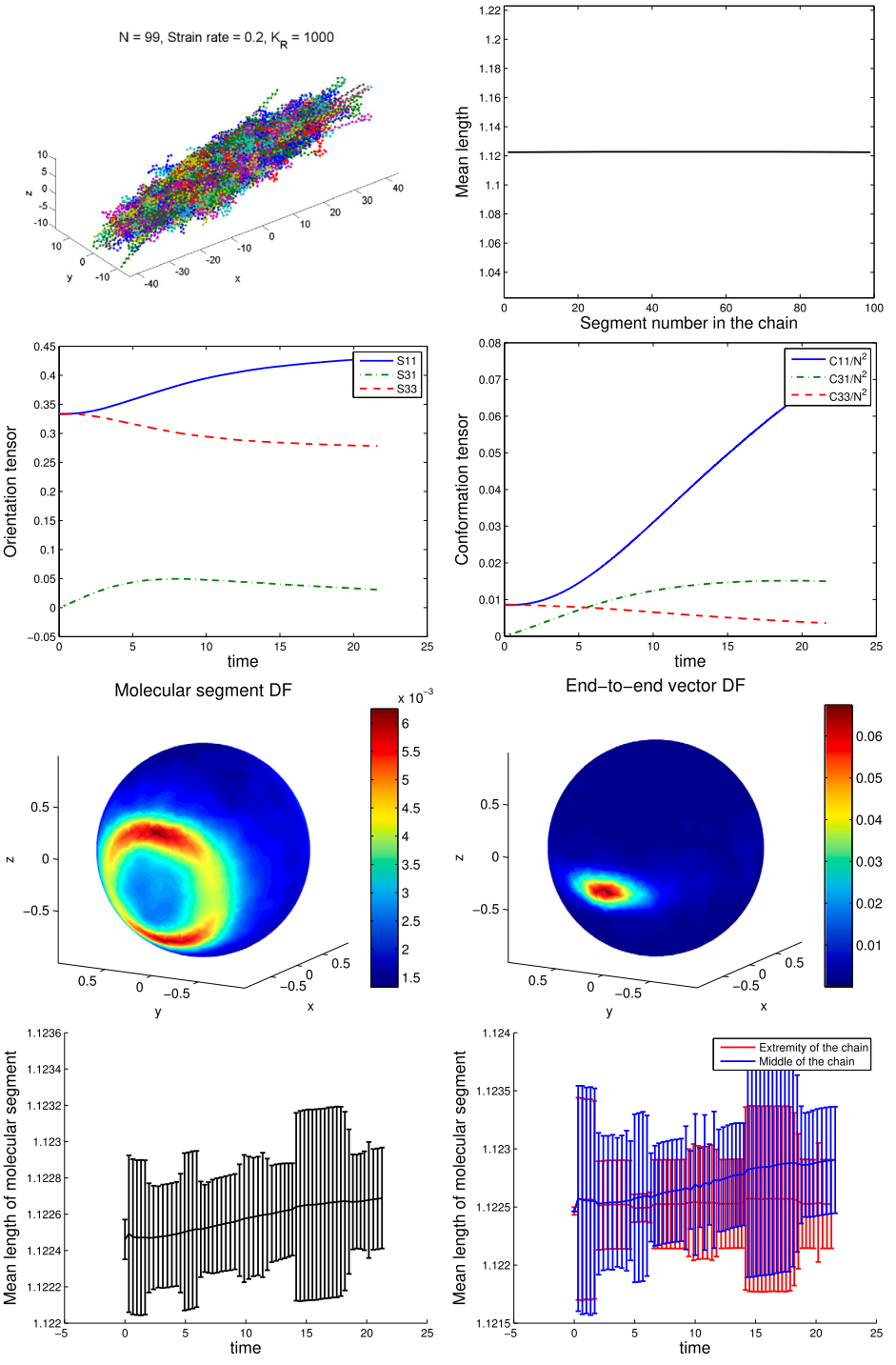

Fig. 6. Shear at $\dot{\epsilon} = 0.2$.

The second contribution of the present work concerns the derivation of an evolution equation for the so-called conformation tensor, that is expected describing the rheological findings, by using artificial intelligence techniques, and in particular deep-learning. It has been proved that the learned model allows deriving very accurate predictions for flows differing from the ones considered in the learning stage (neural network construction).

The obtention of richer expressions of the conformation evolution in general transient and complex flows, as well as the conformation / flow kinematics coupling through an adequate constitutive equation, constitute the main works in progress.

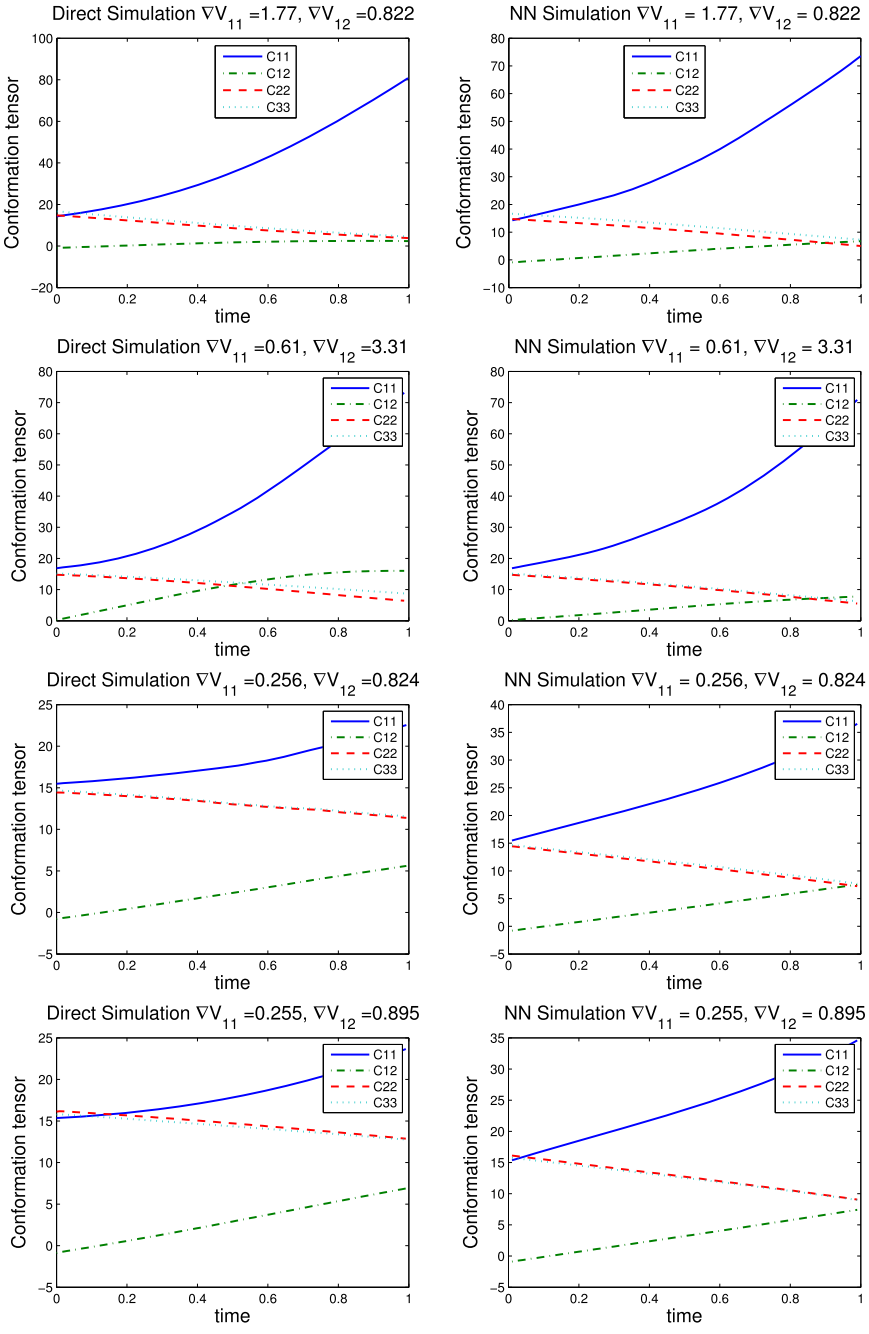

Fig. 7. Comparing direct numerical solutions (left) and neural-network based prediction (right).

Acknowledgements

The authors gratefully acknowledge the ANR ("Agence nationale de la recherche", France) for its support through project AAPG2018 *DataBEST*.

References

[1] C. Binetruy, F. Chinesta, R. Keunings, Flows in Polymers, Reinforced Polymers and Composites. A Multiscale Approach, SpringerBriefs, Springer, 2015.
[2] F. Chinesta, E. Abisset, A Journey Around the Different Scales Involved in the Description of Matter and Complex Systems, SpringerBriefs, Springer, 2017.
[3] G. Ianniruberto, G. Marrucci, Flow-induced orientation and stretching of entangled polymers, Philos. Trans. R. Soc. Lond. A 361 (2003) 677–688.
[4] M. Doi, S.F. Edwards, The Theory of Polymer Dynamics, Oxford Sciences Publications, 1986.

[5] R.B. Bird, C.F. Curtiss, R.C. Armstrong, O. Hassager, Dynamics of Polymeric Liquids, Vol. 2: Kinetic Theory, John Wiley & Sons, 1987.
[6] M. Somasi, B. Khomami, N.J. Woo, J.S. Hur, E.S.G. Shaqfeh, Brownian dynamics simulations of bead-rod and bead-spring chains: numerical algorithms and coarse-graining issues, J. Non-Newton. Fluid Mech. 108 (1–3) (2002) 227–255.
[7] G. Venkiteswaran, M. Junk, A QMC approach for high dimensional Fokker-Planck equations modelling polymeric liquids, Math. Comput. Simul. 68 (2005) 43–56.
[8] R. Winkler, P. Reineker, L. Harnau, Models and equilibrium properties of stiff molecular chains, J. Chem. Phys. 101 (9) (1994) 8119–8129.
[9] L. Harnau, R. Winkler, P. Reineker, Dynamic structure factor of semiflexible macromolecules in dilute solution, J. Chem. Phys. 104 (16) (1996) 6255–6258.
[10] W. Paul, G. Smith, D. Yoon, Static and dynamic properties of a n-C100H202 melt from molecular dynamics simulations, Macromolecules 30 (1997) 7772–7780.
[11] T. Kreer, J. Baschnagel, M. Mueller, K. Binder, Monte Carlo simulation of long chain polymer melts: crossover from Rouse to reptation dynamics, Macromolecules 34 (2001) 1105–1117.
[12] S. Krushev, W. Paul, G. Smith, The role of internal rotational barriers in polymer melt chain dynamics, Macromolecules 35 (2002) 4198–4203.
[13] M. Bulacu, E. van der Gieesen, Effect of bending and torsion rigidity on self-diffusion in polymer melts: a molecular-dynamics study, J. Chem. Phys. 123 (2005) 114901.
[14] M.O. Steinhauser, Static and dynamic scaling of semiflexible polymer chains – a molecular dynamics simulation study of single chains and meltsMech, Time-Depend. Mater. 12 (2008) 291–312.
[15] M. Tanaskovic, L. Fagiano, C. Novara, M. Morari, Data-driven control of nonlinear systems: an on-line direct approach, Automatica 75 (2017) 1–10.
[16] T. Duriez, S. Brunton, B.R. Noack, Machine Learning Control-Taming Nonlinear Dynamics and Turbulence, Springer, 2017.
[17] R.H. Shumway, D.S. Stoer, Time series analysis and its applications, Stud. Inform. Control 9 (4) (2000) 375–376.